NJC

Accepted Manuscript

This is an *Accepted Manuscript*, which has been through the Royal Society of Chemistry peer review process and has been accepted for publication.

Accepted Manuscripts are published online shortly after acceptance, before technical editing, formatting and proof reading. Using this free service, authors can make their results available to the community, in citable form, before we publish the edited article. We will replace this *Accepted Manuscript* with the edited and formatted *Advance Article* as soon as it is available.

You can find more information about *Accepted Manuscripts* in the Information for Authors.

Please note that technical editing may introduce minor changes to the text and/or graphics, which may alter content. The journal's standard Terms & Conditions and the Ethical guidelines still apply. In no event shall the Royal Society of Chemistry be held responsible for any errors or omissions in this *Accepted Manuscript* or any consequences arising from the use of any information it contains.

ROYAL SOCIETY OF CHEMISTRY

www.rsc.org/njc

New Journal of Chemistry

RSCPublishing

ARTICLE

Towards a Potential 4,4'-(1,2,4,5-Tetrazine-3,6-diyl) dibenzoic Spacer to Construct Metal-Organic Frameworks

Cite this: DOI: 10.1039/x0xx00000x

Received 00th January 201X,
Accepted 00th January 201X

DOI: 10.1039/x0xx00000x

www.rsc.org/

Antonio J. Calahorro,[a] Belén Fernández,[a] Celeste García-Gallarín,[b] Manuel Melguizo,[b] David Fairen-Jimenez*[,c] Guillermo Zaragoza,[d] Alfonso Salinas-Castillo,[e] Santiago Gómez-Ruiz[f] and Antonio Rodríguez-Diéguez.[a,*]

The ligand, 4,4'-(1,2,4,5-tetrazine-3,6-diyl)dibenzoic acid has been designed and explored with the aim of using it as linker to construct three-dimensional metal-organic frameworks (MOFs). We have been successful in the formation of a potassium 3D-MOF with this novel linker. This compound is a three-dimensional structure where the layers formed by potassium ions and carboxylate groups are separated by this organic ligand. Luminescence and cytotoxicity studies have been performed. We have used molecular simulations to predict the porous properties of an isoreticular, analogue to IRMOF-16 based on this linker due to the similarity of the new designed ligand with p-terphenyl-4,4''-dicarboxylate present in IRMOF-16.

Introduction

Design of coordination polymers has attracted great attention for their potential applications in the fields of luminescence, gas adsorption, catalysis, magnetic behaviour, electrical conductivity, and drug delivery.[1] These efforts towards the development of new materials have turned in the last years to metal-organic frameworks (MOFs) due to their structural diversity and functional properties.[2] MOFs are mostly constructed from clusters of transition-metal ions held in position in a lattice by ligation to organic molecules.[3] Recently, we have designed a new symmetrically multidentate bridging ligand, 3,3'-(1,2,4,5-tetrazine-3,6-diyl)dibenzoic acid and some MOFs with interesting luminescence, magnetic and adsorption properties.[4] In this context, and as part of our continuing studies on tetrazine derivative ligands, we have designed the novel 4,4'-(1,2,4,5-tetrazine-3,6-diyl)dibenzoic acid (**1**) ($H_2$44dbtz), which contains two benzoic groups donors, bonding to the metals, and a central tetrazine π-acceptor function. Our idea stems from the use of 3,6-disubstituted-1,2,4,5-tetrazine moieties, who have become popular as efficient electronic spacers in dinuclear and polynuclear systems.[5] This is primarily due to the fact that the tetrazine-based low-lying π* orbital conveys strong p-accepting characteristics. Another reason to design this ligand was to improve the adsorption properties of IRMOF-16 (made with p-terphenyl-4,4''-dicarboxylate), due to the similarity of **1** with the linker used by Yaghi and co-workers.[6] Herein, we report the synthetic, structural, luminescence and cytotoxicity properties of this new ligand, shown in Scheme I, and the first example of the coordination polymer $[K_2(44dbtz)]_n$ (**2**) obtained with it. We choose potassium as a metal with the idea of developing new materials with electronic conductivity and biocompatibility for drug delivery applications. Using molecular simulations, we then extended the use of this ligand into two new potential MOFs that can be built with **1**. The molecular simulations are based on the Zn-based IRMOF family due to the similarity of **1** with the ligand present in IRMOF-16. To the best of our knowledge, this is the first time that this linker and MOFs have been explored.

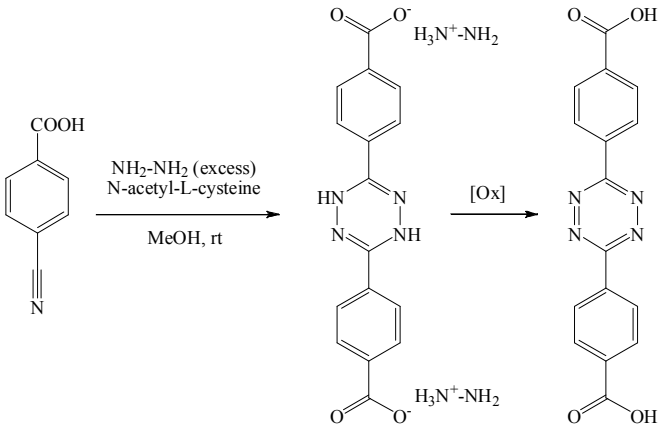

Scheme I. Preparation of 4,4'-(1,2,4,5-tetrazine-3,6-diyl)dibenzoic acid.

Results and Discussion

The main aim of this paper is the synthesis of 4,4'-(1,2,4,5-tetrazine-3,6-diyl)dibenzoic acid. It was performed following a variant of the classical Pinner-type scheme in two steps. Firstly, the reaction between 4-cyanobenzoic acid and excess hydrazine catalysed by N-acetylcysteine under inert atmosphere renders the dihydrotetrazine derivative. Secondly, the dihydrotetrazine derivative was oxidized to give the desired fully aromatic compound 4,4'-(1,2,4,5-tetrazine-3,6-diyl)dibenzoic acid (**1**) by simple stirring a methanol suspension of the dihydroderivative under air atmosphere. **1** was characterized by 1H NMR, 13C NMR and X-ray diffraction (see ESI).

Description of the structures.

Compound **1** crystallizes in the monoclinic space group $P2_1/n$; the asymmetric unit consisting of medium $H_2$44dbtz ligand that grows by symmetry generated an almost linear alignment between the aromatic rings and the terminal carboxylate groups (dihedral angles, 7.76-8.49º) and one crystallization dimethyl-sulfoxide molecule. In the $H_2$44dbtz unit (Figure 1), the bond distances and angles are very similar to those expected in the tetrazine and benzene rings of 3,3'-(1,2,4,5-tetrazine-3,6-diyl)dibenzoic acid.[4a] In the structure there is only one type of hydrogen bond (Figure S1), yielding a three-nuclear unit formed by one central $H_2$44dbtz unit and two dimethyl-sulfoxide molecules in which oxygen atom pertaining to dimethyl-sulfoxide and the oxygen from the carboxylate group are involved (O1-H…O3 = 2.587 Å). These three-nuclear units are packed thought stacking interactions (3.531(5) Å) among the tetrazine with the benzene rings and (3.699(5) Å) the benzene-benzene rings of neighbour units (Figure S2).

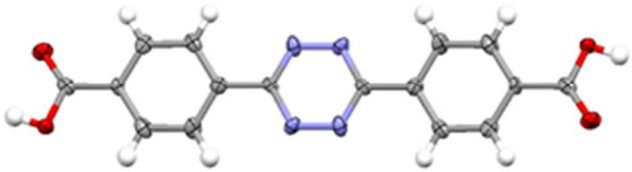

Figure 1. Crystalline structure of 4,4'-(1,2,4,5-tetrazine-3,6-diyl)dibenzoic acid. Carbon atoms, grey; nitrogen, blue; oxygen, red; hydrogen, white. Dimethyl-sulfoxide molecule has been omitted for clarity. Thermal ellipsoids are drawn at the 50% probability level.

Hydrothermal reaction of KOH (0.1 mmol) with $H_2$44dbtz (0.1 mmol) in water:acetonitrile (5 ml) at 140 ºC for 36 h followed by cooling to room temperature yields prismatic pink crystals of **2** (in 61% yield). The crystal structures of **1** and **2** were determined by single crystal X-ray crystallography. Table 1, S2 and S3 give the detail refinements, main bond lengths and angles of the structures, respectively (ESI).

Compound **2** is a three-dimensional coordination polymer where the asymmetric unit is formed by half potassium atom with distorted coordination geometry and half $H_2$44dbtz ligand. In the structure, the cationic ion stabilizes its charge with the monoanic ligand where only one carboxylate group is deprotonated. The coordination mode of 44dbtz anionic ligand in **2** is shown in Figure 2. Each linker binds to eight potassium atoms in a quad-bidentate bridging fashion. Potassium atoms exhibit very distorted KO_8 geometries (Figure S3, up) with the oxygen atoms pertaining to carboxylate groups pertaining to eight different 44dbtz$^-$ ligands, showing bond distances of K-O range from 2.693(2) to 3.143(2) Å and O–K–O angles varying from 45.84° to 152.12°. Carboxylate oxygen links the K centres to form 2D sheets, which runs parallel to the *ab* plane (Figure S3, bottom).

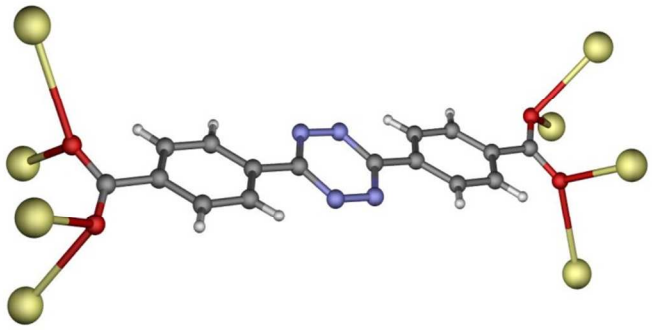

Figure 2. A view of the coordination mode of the ligand in **2**.

The 2D layer consists of KO_8 polyhedron that are corner-shared to form the layered structure, in which the distance between the potassium atoms is 4.135 Å. These layers, 14.094 Å apart, stack along the [001] direction and are separated by the 44dbtz ligand with the aromatic rings layered along the [010] direction. The distance between two consecutive aromatic rings are on the average 4.5 Å in the [100] direction. The linear 44dbtz ligands along the *c* axis act as a pillar and serve to link adjacent layers to form an extended 3D coordination network as indicated in Figure 3. Unfortunately, the adjacent pillars are too close to each other, and therefore there is no accessible void in **2**.

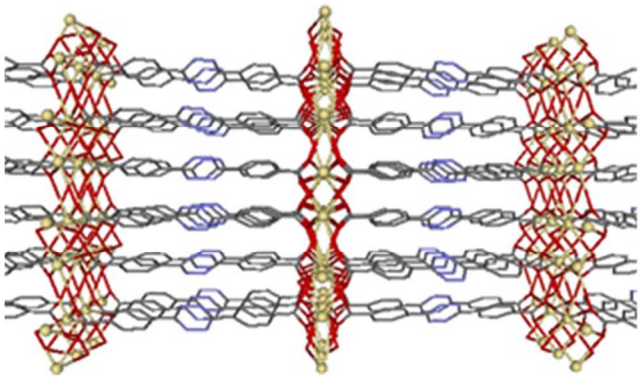

Figure 3. View down the *b* axis of the structure in the three-dimensional network. Carbon atoms, grey; nitrogen, bue; oxygen, red; potassium, yellow. Hydrogen atoms have been omitted for clarity.

Luminescence Properties.

Thanks to its extended aromaticity and to the presence of polyheterosubstituded hexa-atomic rings, $H_2$44dbtz is a good

candidate for enhanced emissive properties, tuneable, in principle, by coordination to different metals or environments. Figure 4 shows the emission spectra of compounds **1** and **2** in solid state at room temperature.

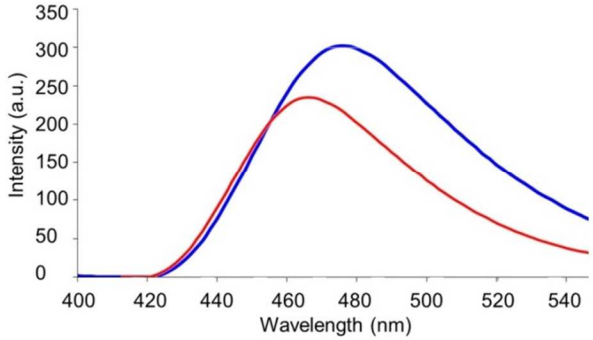

Figure 4. The emission spectra of **1** (red line) and **2** (blue line) in solid state at room temperature.

The emission spectrum of **1** and **2** at room temperature in solid state exhibited broad intense emission bands centred about 463 and 476 nm, respectively, upon excitation at 310 nm. The emissions in **2** is assigned to intraligand π–π* transitions, although a considerable red-shift is observed with respect to the **1** emission band. Moreover, the emission is more intense than that of the free ligand, which may be explained in terms of the rigidity. Indeed, the rigidity of the coordinated ligand reduces the loss of energy, thereby increasing the emission efficiency.

Adsorption Properties.

Following the synthesis of this first K-based MOF, we used molecular simulations to study the potential of this ligand to build new MOFs. We choose IRMOF-16 as analogue example to build a new isoreticular structure due to the similarity of the new designed ligand **1** with p-terphenyl-4,4''-dicarboxylate present in IRMOF-16.

The strategy to build the new structures is similar to the scheme we described in previous papers.[11] We started with the asymmetric unit of IRMOF-16 and substituted the central carbon atoms by nitrogen. After using symmetry operations we built the new IRMOF-16 based structure, **3**. In addition, a catenated version was built, creating a new structure, **4**. The unit cells of both structures were then subject to geometry optimization based on molecular mechanics, modifying the size of the unit cell and the atomic coordinates of the new structures. Once the models have been obtained, we calculated then the N_2 and CO_2 adsorption isotherms at 77 and 298 K, respectively, using grand canonical Monte Carlo (GCMC) simulations to predict their potential adsorption performance. Figure 5 shows the simulated isotherms. N_2 isotherms of the non-catenated and catenated MOFs are typical of meso- and microporous materials, respectively. The calculated BET areas were 5390 and 4620 m^2/g for **3** and **4**, respectively. In the case of CO_2, both structures show Type V adsorption isotherms.

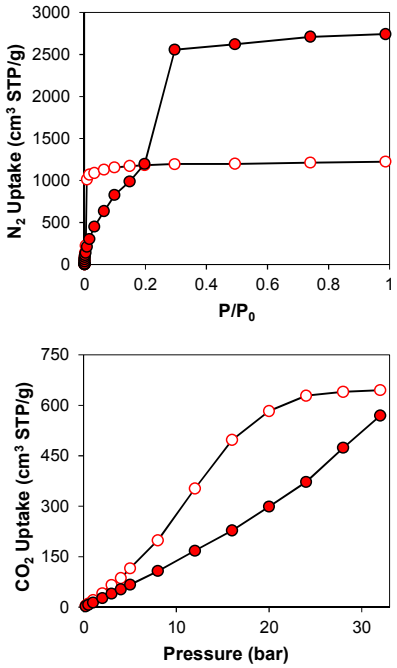

Figure 5. Adsorption isotherms of N_2 (top) and CO_2 (bottom) on 3, closed red circles, and 4, open red circles.

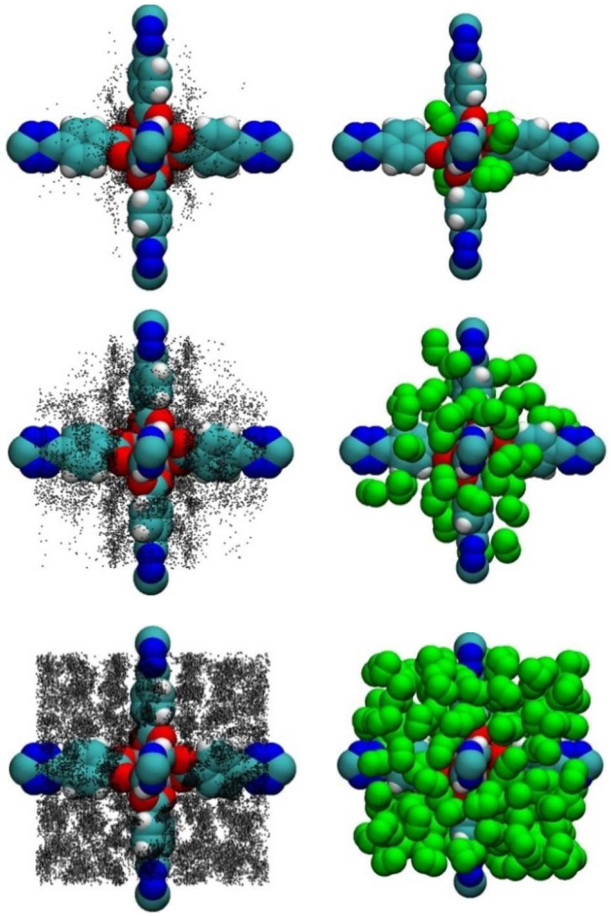

Figure 6. Density distributions (left) and snapshots (right) of N_2 adsorption on 3 at 77 K at (from top to bottom) low, medium and high loadings, obtained by GCMC. Black points and green spheres represent the N_2 molecules in the density distributions and snapshots, respectively.

We have shown previously that the existence of Type V – sigmoid shapes in adsorption isotherms is related to weak MOF-gas interactions compared with gas-gas interactions, which stems in this case from the open porosity of these structures. Figures 6, S4 and S5 show the adsorption mechanism of N_2 and CO_2 in structures **3** and **4** through the representation of snapshots and density distributions. Gas molecules are first adsorbed close to the metal cluster before being adsorbed along the linkers and then in the rest of the porosity.

Cytotoxicity Studies

In addition to the gas adsorption, a relatively new – and very promising – application for MOFs is the use of these materials for drug delivery. In this case, the cytotoxicity of the MOF and its building blocks is key to evaluate the potential of the materials that can be built. For drug delivery, water stability of a MOF is very important. Eventually, the MOF will be dissolved in the body and the building blocks (i.e. the metal and organic ligand) may interact or not with existing cell pathways. We have therefore studied the biocompatibility of the isolated ligand **1** in order to provide further information about the potential of this linker in drug delivery. We evaluated the *in vitro* cytotoxicity of cells exposed to compound **1** in the human embryonic kidney cell line (HEK293) at different concentrations and a wide range of incubation times (Figure 7). The results obtained show that for long incubation times and at the highest concentrations analysed apparent mild signs of toxicity appeared. This can be considered negligible, with cell viability greater than 80-85%.

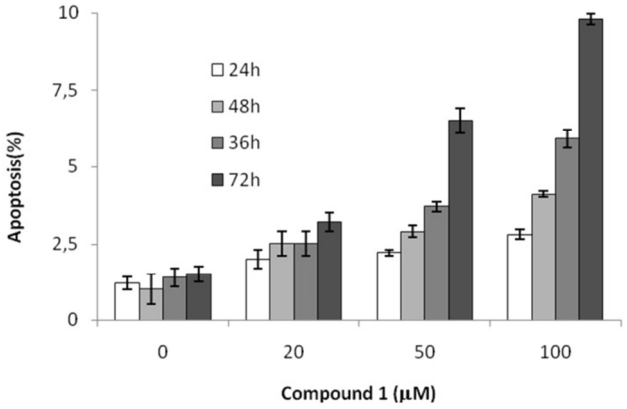

Figure 7. Concentration-time toxicity dependence of HEK293 cells exposed to compound 1. Quantification from three different experiments (mean+s.e.m. (n = 3); * P >0.05.

Conclusions

The main aim of this paper was the design of the novel 4,4'-(1,2,4,5-tetrazine-3,6-diyl)dibenzoic acid ligand. We also show the synthesis of a new metal-organic framework based in potassium metal centres, as well as the luminescent properties of both the ligand and the K-based MOF. Indeed, the extended aromaticity and the presence of poly-heterosubstituded hexa-atomic rings in this ligand, makes it a good candidate for enhanced emissive properties. We continued with the design of hypothetical MOFs analogues to IRMOF-16 due to the similarity in the ligands, and the study of their adsorption properties using molecular simulations. We conclude showing the low toxicity of the proposed ligand, which makes it interesting for drug delivery applications. Work along this line using other paramagnetic/lanthanides metals and XRD measurements under high pressure are in progress in our lab.

Experimental Section

General Procedures: Unless otherwise stated, all reactions were conducted by hydrothermal conditions, with the reagents purchased commercially and used without further purification.

Synthesis of 4,4'-(1,2,4,5-tetrazine-3,6-diyl)dibenzoic acid (1)

Hydrazine hydrate (1,32 mL, 27,2 mmol) was dropwise added to a solution of 4-cyanobenzoic acid (1.000 g, 6.8 mmol) and N-acetyl-L-cysteine (1.115g, 6.8 mmol) in MeOH (12.5 mL ml) at room temperature under Ar atmosphere, and the resulting mixture was stirred at room temperature for 5 days under Ar atmosphere. Then, the yellowish solid in suspension was collected by filtration, washed with methanol (3x30 ml) and dried under vacuum to afford 1.21 g (3.1 mmol, 92%) (2). 1H NMR (400 MHz, DMSO-d6) δ ppm 7.93 (4 H, d, J=8.70 Hz) 7.99 (4 H, d, J=8.50 Hz) 8.13 (10 H, br. s.) 9.29 (2 H, s). 13C NMR (101 MHz, DMSO-d6) δ ppm 126.12, 129.40, 132.04, 133.90, 147.12, 166.71.13C NMR (125.7 MHz, solid state CP-MAS-TOSS) δ ppm 121.2-133.0, 148.0. The intermediate tetrazine was resuspended in MeOH (25 ml). An H2O2 solution(20 ml, 10 volume) was dropwise addedto the methanolic solution and kept under stirring in an open round-bottomed flask at room temperature for 24 h. Then, the violet solid in suspension was collected by filtration, washed with methanol (40 ml) and treated with a methanolic solution of sulfuric acid (3% p/v) at room temperature for 24 h. The purple solid in suspension was collected by filtration, washed withmethanolic solution of sulfuric acid (0.5% p/v) and methanol (3 x 40 ml) and, finally, dried under vacuum to afford 0.935 g (2.9 mmol, 85%) of 4,4'-(1,2,4,5-tetrazine-3,6-diyl)dibenzoic acid.Furthermore, to obtain suitable x-ray quality crystals, 0.01 mmol (3.2mg) of 4,4'-(1,2,4,5-tetrazine-3,6-diyl)dibenzoic acid were solved in DMSO, obtaining violet crystals after one week.13C NMR (125.7 MHz, solid state CP-MAS-TOSS) δ ppm 124.2-137.0, 161.7, 171.8.

Synthesis of $[K_2(dbtz)]n$ (2)

A mixture of H2dbtz (32.2 mg, 0.1 mmol), KOH (29.75 mg, 0.1 mmol) and a water:acetonitrile (1:1) mixture (5 mL) was placed in a Teflon reactor (23 mL) and heated at 140 °C for 3 d. After the mixture was cooled to room temperature at a rate of 15 °C•h^{-1}, the solution was filtered and left at room temperature, obtaining dark pink crystals of 2 after three days, with a yield of 61% (based on K). $C_{16}H_8N_4O_4K_2$ (Mr = 398.46): calcd. C

48.23, H 2.02, N 14.06; found C 48.44, H 2.21, N 13.89. IR: = 1610 (m), 1592 (m), 1546 (s), 1529 (s), 1455 (s), 1422 (s), 1387 (s), 776(m) cm^{-1}.

Physical measurements

Elemental analyses were carried out at the "Centro de Instrumentación Científica" (University of Granada) on a Fisons Carlo Erba analyser model EA 1108. IR spectra on powdered samples were recorded with a ThermoNicolet IR200FTIR using KBr pellets.

Single-Crystal Structure Determination.

Suitable crystals of **1** and **2** were mounted on a glass fibre and used for data collection on a Bruker AXS APEX CCD area detector (λ = 0.71073 and 1.54178 Å for **1** and **2**, respectively) by applying the w-scan method. Lorentz-polarization and empirical absorption corrections were applied. The structures were solved by direct methods and refined with full-matrix least-squares calculations on F^2 using the program SHELXS97. Anisotropic temperature factors were assigned to all atoms except for hydrogen atoms, which are riding their parent atoms with an isotropic temperature factor arbitrarily chosen as 1.2 times that of the respective parent. In general, the quality of data is very low, several crystals of **1** and **2** were measured and the structure was solved from the best data we were able to collect. Final R(F), wR(F2) and goodness of fit agreement factors, details on the data collection and analysis can be found in Table 1. Selected bond lengths and angles are given in Tables S1 and S2. CCDC reference numbers for the structures were 1030582-1030583. Copies of the data can be obtained free of charge upon application to CCDC, 12 Union Road, Cambridge CB2 1EZ, U.K. (fax, (+44)1223 336-033; e-mail, deposit@ ccdc.cam.ac.uk).

Luminescence measurements.

A Varian Cary-Eclipse Fluorescence Spectrofluorimeter was used to record the fluorescence spectra. The spectrofluorimeter was equipped with a xenon discharge lamp (peak power equivalent to 75 kW), Czerny-Turner monochromators, R-928 photomultiplier tube which is red sensitive (even 900 nm) with manual or automatic voltage controlled using the Cary Eclipse software for Windows 95/98/NT system. The photomultiplier detector voltage was 700 V and the instrument excitation and emission slits were set at 5 and 5 nm, respectively. .

Structure prediction.

The structures of **3** and **4** were modeled using the structure of the original cubic IRMOF-16 ($a = b = c$ = 21.4903 Å, *Im3m*) and incorporating the nitrogen atoms in the central aromatic ring of the ligand. The structure was then subject to geometry optimization, without any symmetry constrains using *P1*, based on molecular mechanics calculations. This procedure allows the modification of the position of all the atoms in the structure in order to minimize the energy. These calculations were performed with the Forcite module of Materials Studio, using

Table 1. Crystallographic Data and Structural Refinement Details

compound	1	2
chemical formula	$C_{20}H_{22}N_4O_6S$	$C_{16}H_9N_4O_4K$
CCDC	1030582	1030583
M/gmol^{-1}	478.56	360.37
T (K)	100	100
λ/Å	0.71073	1.54178
cryst syst	monoclinic	monoclinic
space group	*P21/n*	*I2/a*
a/ Å	7.315(4)	5.970(1)
b/ Å	7.088(4)	6.738(1)
c/ Å	20.776(13)	34.50(1)
β/deg	90.069(18)	94.68(5)
V/ Å^3	1077.3(11)	1383.2(5)
Z	2	4
ρ(g cm-3)	1.475	1.731
μ(mm-1)	0.294	3.688
Unique reflections	4536	2558
R(*int*)	0.104	0.042
GOF on F^2	1.016	1.148
R1 [$I > 2\sigma(I)$] [a]	0.060	0.041
wR2 [$I > 2\sigma(I)$] [a]	0.138	0.097

[a] $R(F) = \sum||F_o| - |F_c||/\sum|F_o|$; $wR(F^2) = [\sum w(F_o^2 - F_c^2)^2/\sum wF^4]^{1/2}$

an algorithm that is a cascade of the steepest descent, adjusted basis set Newton-Raphson, and quasi-Newton methods. The bonded and the short range (van der Waals) non-bonded interactions between the atoms were modeled using the Universal Force Field. A cutoff distance of 12 Å was used for the LJ interactions during the geometry optimization. The long range, electrostatic, interactions, due to the presence of partial atomic charges, were modeled using a Coulombic term. The Ewald sum method was used to compute the electrostatic interactions. Partial atomic charges were derived from the charge equilibration method (QEq) as implemented in Forcite.

Gas adsorption simulation

The adsorption of N_2 was investigated using grand canonical Monte Carlo (GCMC) simulations implemented in RASPA. We used an atomistic model for the MOF structures, in which the framework atoms were kept fixed at the crystallographic positions. We used the standard Lennard-Jones (LJ) 12-6 potential to model the interactions between the framework and the gases. Apart from the LJ, we included a Coulomb potential. The parameters for the framework atoms were obtained from the UFF force field. N_2 and CO_2 were modeled using the TraPPE potential with charges placed on each atom and at the center of mass. Partial atomic charges of the MOF were derived from the charge equilibration method (QEq). The Lorentz-Berthelot mixing rules were employed to calculate fluid-solid parameters. LJ interactions beyond 18 Å were neglected. 107 Monte Carlo steps were performed, the first 50% of which were used for equilibration, and the remaining steps were used to calculate the ensemble averages. To calculate the gas-phase fugacity we used the Peng-Robinson equation of state. After

equilibration, density distributions were obtained by storing the center of mass positions of all the adsorbed molecules at regular intervals during the simulation. These density distributions provide valuable information about the preferential adsorption sites and the local spatial disorder of the adsorbed molecules. Snapshots represent one single molecular configuration during the simulation.

Acknowledgements

This work was supported by the MEC of Spain (Project CTQ2011-24478) and the Junta de Andalucía (FQM-1484). D.F.-J. thanks the Royal Society for a University Research Fellowship.

Notes and references

a Departamento de Química Inorgánica, Universidad de Granada, 18071, Granada, Spain. Tel: 0034958240442; E-mail: antonio5@ugr.es
b Departamento de Química Inorgánica y Orgánica, Universidad de Jaén, Campus Las Lagunillas, 23071, Jaén, Spain.
c Dept. of Chemical Engineering & Biotechnology, University of Cambridge, United Kingdom. E-mail: df334@cam.ac.uk
d Unidad de Rayos X; RIAIDT Edificio CACTUS, Universidad de Santiago de Compostela, 15782 Santiago de Compostela, Spain.
e Departamento de Química Analítica, Universidad de Granada, 18071, Granada, Spain
f Departmento de Biología y Geología, física y Química Inorgánica, E.S.C.E.T., Universidad Rey Juan Carlos, c/ Tulipán s/n, 28933 Móstoles, Spain.

† Electronic Supplementary Information (ESI) available: [Crystal Data, Coordination Environments of Metal Ions, Gas Adsorption Simulations and Computational Structural Characterization, Gas Adsorption Measurements and Luminescence Properties]. CCDC reference numbers are 1030582-1030583 for **1** and **2**, respectively. For crystallographic data in CIF format see DOI.

1.- (a) L. Hou L, D. Li, *Inorg. Chem. Commun*. 2005, **8**, 190; (b) S. L. Qiu, G. S. Zhu, *Coord. Chem. Rev*. 2009, **253**, 2891; (c) J.J. Perry IV, J. A. Perman, M. J. Zaworotko, *Chem. Soc. Rev*. 2009, **38**, 1400; (d) S. Natarajan, P. Mahata, Chem. Soc. Rev. 2009, 38, 2304. (e) M. Wriedt, A. A. Yakovenko, G. J. Halder, A. V. Prosvirin, K. R. Dunbar and H.-C. Zhou, *J. Am. Chem. Soc*., 2013, **135**, 4040; (f) S. Shimomura, M. Higuchi, R. Matsuda, K. Yoneda, Y. Hijikata, Y. Kubota, Y. Mita, J. Kim, M. Takata and S. Kitagawa, *Nat. Chem*., 2010, **2**, 633; (g) Y. Zhang, X. Bo, C. Luhana, H. Wang, M. Li and L. Guo, *Chem. Commun*., 2013, **49**, 6885; (h) Y.-W. Li, J.-R. Li, L.-F. Wang, B.-Y. Zhou, Q. Chen and X.-H. Bu, *J. Mater. Chem. A*, 2013, **1**, 495; (i) María C. Bernini, David Fairen-Jimenez, Marcelo Pasinetti, Antonio J. Ramirez-Pastor and Randall Q. Snurr, *J. Mater. Chem. B*, 2014, **2**, 766.

2.- (a) H.-C. Zhou, J.R. Long and O.M. Yaghi, *Chem. Rev*. 2012, **112**, 673; (b) D. Tian, Y. Li, R.-Y. Chen, Z. Chang, G.-Y. Wang and X.-H. Bu, *J. Mater. Chem. A*, 2014, **2**, 1465; (c) A. U. Czaja, N. Trukhan and U. Muller, *Chem. Soc. Rev*., 2009, **38**, 1284; (d) J. Della Rocca, D. Liu and W. Lin, *Acc. Chem. Res*., 2011, **44**, 957; (e) A. C. McKinlay, R. E. Morris, P. Horcajada, G. Ferey, R. Gref, P. Couvreur and C. Serre, *Angew. Chem., Int. Ed*., 2010, **49**, 6260; (f) J. S. Seo, D. Whang, H. Lee, S. I. Jun, J. Oh, Y. J. Jeon and K. Kim, *Nature (London)*, 2000, **404**, 982; (g) Q. Zhou, F. Yang, B. Xin, G. Zeng, X. Zhou, K. Liu, D. Ma, G. Li, Z. Shi and S. Feng, *Chem. Commun*., 2013, **49**, 8244

3.- (a) T.R. Cook, Y.-R. Zheng and P.J. Stang, *Chem. Rev*. 2013, **113**, 734. (b) M. Eddaoudi, D. B. Moler, H. Li, B. Chen, T. M. Reineke, M. O'Keeffe and O. M. Yaghi, *Acc Chem Res*, 2001, **34**, 319; (c) Y.-Q. Lan, S.-L. Li, H.-L. Jiang and Q. Xu, *Chem.- Eur. J*., 2012, **18**, 8076; (d) O. K. Farha, C. D. Malliakas, M. G. Kanatzidis and J. T. Hupp, *J. Am. Chem. Soc*., 2010, **132**, 950; (e) D. N. Dybtsev, M. P. Yutkin, D. G. Samsonenko, V. P. Fedin, A. L. Nuzhdin, A. A. Bezrukov, K. P. Bryliakov, E. P. Talsi, R. V. Belosludov, H. Mizuseki, Y. Kawazoe, O. S. Subbotin and V. R. Belosludov, *Chem.-Eur. J*., 2010, **16**, 10348

4.- (a) A. J. Calahorro, A. Peñas-Sanjuan, M. Melguizo, D. Fairen-Jimenez, G. Zaragoza, B. Fernández, A. Salinas-Castillo, and A. Rodríguez-Diéguez, *Inorg.Chem*. 2013, **52**, 546. (b) A. J. Calahorro, A. Salinas-Castillo, J. M. Seco, J. Zuniga, E. Colacio and A. Rodriguez-Dieguez, *CrystEngComm*, 2013, **15**, 7636; (c) J. M. Seco, D. Fairen-Jimenez, A. J. Calahorro, L. Mendez-Linan, M. Perez-Mendoza, N. Casati, E. Colacio and A. Rodriguez-Dieguez, *Chem. Commun.*, 2013, **49**, 11329; (d) A. J. Calahorro, P. Macchi, A. Salinas-Castillo, E. S. Sebastian, J. M. Seco and A. Rodriguez-Dieguez, *CrystEngComm*, 2014, **16**, 10492

5.- W. Kaim, Coord. Chem. Rev. 2002, 230, 127.; (b) Z.-Z. Lu, R. Zhang, Y.-Z. Li, Z.-J. Guo and H.-G. Zheng, J. Am. Chem. Soc., 2011, 133, 4172; (c) Z. Chang, D.-S. Zhang, Q. Chen, R.-F. Li, T.-L. Hu and X.-H. Bu, *Inorg. Chem*., 2011, **50**, 7555

6.- M. Eddaoudi, J.Kim, N. Rosi, D. Vodak, J. Wachter, M. O´Keeffe and O. Yaghi, *Science*, 2002, **295**, 469.

7.- (a) R.A. Smaldone, R.S. Forgan, H. Furukawa , J.J. Gassensmith, A.M.Z. Slawin, O.M. Yaghi and J.F. Stoddart, *Angew. Chem., Int. Ed.*, 2010, **49**, 8630; (b) R.S. Forgan, R.A. Smaldone, J.J. Gassensmith, H. Furukawa, D.B. Cordes, Q. Li, C.E. Wilmer, Y.Y. Botros, R.Q. Snurr, A.M.Z. Slawin and J. F. Stoddart, *J. Am. Chem. Soc*., 2012, **134**, 406.

8.- (a) M. Huang, U. Schilde, M. Kumke, M. Antonietti and H. Cölfen, *J. Am. Chem. Soc.*, 2010, **132**, 3700; (b) M.C. Bernini, D. Fairen-Jimenez, M. Pasinetti, A.J. Ramirez-Pastor, R.Q. Snurr, *J. Mater. Chem. B*, 2014, **2**, 766.

9.- A. Pinner, J.A. Liebig, *Chem*. 1897, **297**, 221.

10.- (a) S. Aldridge, A.J. Downs; The Group 13 Metals Aluminium, Gallium, Indium and Thallium, , Ed.: John Wiley & Sons , 2011; (b) A. Rodríguez-Diéguez, A. Salinas-Castillo, A. Sironi, J.M. Seco and E. Colacio, *CrystEngComm*, 2010, **12**, 1876. (c) B. Tan, Z.-L. Xie, M.-L. Feng, B. Hu, Z.-F. Wu and X.-Y. Huang, *Dalton Trans*., 2012, **41**, 10576.

11.- (a) D. Fairen-Jimenez, Y.J. Colón, O.K. Farha, Y.-S. Bae, J.T. Hupp and R.Q. Snurr, *Chem. Commun*., 2012, **48**, 10496; (b) W. Bury, D. Fairen-Jimenez, M.B. Lalonde, R.Q. Snurr, O.K. Farha and J.T. Hupp, *Chem. Mater*., 2013, **25**, 739; (c) R.S. Forgan, R.J. Marshall, M. Struckmann, A.B. Bleine, D.-L. Long, M.C. Bernini and D. Fairen-Jimenez, *CrystEngComm*, 2015, **17**, 299.

12.- (a) D. Frenkel and B. Smit, Understanding Molecular Simulations: From Algorithms to Applications, Academic Press, San Diego, 2nd edn, 2002.

13.- D. Fairen-Jimenez, N. A. Seaton and T. Düren, *Langmuir*, 2010, **26**, 14694.